 CMC, vol.11, no.3, pp.185-208, 2009

The Method of Fundamental Solutions for One-Dimensional Wave Equations

Gu, M. H.[1], **Young, D. L.**[1,2] **and Fan, C. M.**[1]

Abstract: A meshless numerical algorithm is developed for the solutions of one-dimensional wave equations in this paper. The proposed numerical scheme is constructed by the Eulerian-Lagrangian method of fundamental solutions (ELMFS) together with the D'Alembert formulation. The D'Alembert formulation is used to avoid the difficulty to constitute the linear algebraic system by using the ELMFS in dealing with the initial conditions and time-evolution. Moreover the ELMFS based on the Eulerian-Lagrangian method (ELM) and the method of fundamental solutions (MFS) is a truly meshless and quadrature-free numerical method. In this proposed wave model, the one-dimensional wave equation is reduced to an implicit form of two advection equations by the D'Alembert formulation. Solutions of advection equations are then approximated by the ELMFS with exceptionally small diffusion effects. We will consider five numerical examples to test the capability of the wave model in finite and infinite domains. Namely, the traveling wave propagation, the time-space Cauchy problems and the problems of vibrating string, etc. Numerical validations of the robustness and the accuracy of the proposed method have demonstrated that the proposed meshless numerical model is a highly accurate and efficient scheme for solving one-dimensional wave equations.

Keywords: Eulerian-Lagrangian method of fundamental solutions, D'Alembert formulation, one-dimensional wave equations, meshless numerical method

1 Introduction

After tremendous progress of the computer science technology, the developments of highly accurate and efficient wave solvers still remain an important and challenging research topic nowadays in the computational physics. The wave equations govern many interesting physical science problems such as the stress wave in an elastic solid, water wave propagation in water bodies, scattering problems of elec-

[1] Department of Civil Engineering, National Taiwan University, Taipei, 10617, Taiwan
[2] Corresponding author. E-mail: dlyoung@ntu.edu.tw; Tel and Fax: +886-2-2362-6114

tromagnetic waves and sound wave propagation in a medium, etc. Although there are many conventional mesh-dependent numerical methods available for solving hyperbolic-type partial differential equations like wave equations, however there is still very limited works in this area as far as meshless numerical schemes are concerned. Therefore in this study, we will construct a meshless numerical model to solve the wave equations in one-dimensional time-space domain based on the ELMFS and the D'Alembert formulation.

In general the so-called meshless or meshfree numerical methods can be roughly classified into domain-type and boundary-type methods. The famous meshless domain-type methods such as the meshless local Petrov-Galerkin (MLPG) method (Han and Atluri (2004), Sladek, Sladek, Zhang, Garcia and Wunsche (2006)), the radial basis function collocation method (RBFCM) (Amaziane, Naji and Ouazar (2004), Young, Chen and Wong (2005)), etc. were well developed to solve homogeneous or nonhomogeneous partial differential equations. The well-known meshless boundary-type methods like the MFS (Alves and Antunes (2005)), the hyper-singular meshless method (HMM) (Young, Chen and Lee (2005)) and regularized meshless method (RMM) (Chen, Kao, Chen, Young, and Lu (2006), Chen, Chen, and Kao (2008), Chen, Kao and Chen (2009), Chen, Wu, Kao, and Chen (2009)), etc. were also constructed to obtain the solutions of the homogenous partial differential equations.

The MFS was first used to solve the boundary value problems by the time-independent fundamental solutions (or free-space Green's functions) (Kupradze and Aleksidze (1964), Mathon and Johnston (1977), Golberg (1995)). In those preceding studies, most of works were focused on solving the elliptic-type partial differential equations. Later on the MFS was extended to deal with the parabolic-type problems by the time-dependent fundamental solution. The homogeneous diffusion problems (Young, Tsai, Murugesan, Fan and Chen (2004)), nonhomogeneous diffusion problems (Young, Tsai and Fan (2004)), unsteady Stokes problems (Tsai, Young, Fan and Chen (2006)) and also the unsteady Navier-Stokes equations (Young, Chen, and Fan (2008)) were successfully solved by using the time-dependent MFS formulation.

To solve the more involved advection-diffusion equations we can extend the time-dependent diffusion fundamental solution by combing with the concept of the ELM (also called the method of characteristics). The ELM combining with the boundary element method (BEM) was previously used to solve the multi-dimensional advection-diffusion problems (Young, Wang and Eldho (2000)). However, the mesh generation and numerical quadrature are still needed when the BEM is adopted. The ELM concept is also applied to develop the adaptive particle-based advection scheme (called AMMoC) for building the local mesh free Buckley-Leverett model

(Iske and Käser (2005)). The MFS was combined with the ELM to develop the ELMFS to solve the multi-dimensional advection-diffusion equations (Young, Fan, Tsai, Chen and Murugesan (2006)). The ELMFS was further applied to solve the non-linear Burgers' equations (Young, Fan, Hu and Atluri (2008)) and even the notorious Navier-Stokes equations (Young, Lin, Fan and Chiu (2009)). The ELMFS was also extended to approximate the solutions of the advection equations (Gou and Young (2005)). In the above study, we have proved that the ELMFS is a superior scheme for approximating the solution of the advection equation. The advection-diffusion equation is considered to asymptotically approach the single hyperbolic equation when the extremely small diffusion effects are taken. When the diffusive term becomes very small, the advection-diffusion equation will approximate to the pure advection equation.

Although the MFS can efficiently solve the elliptic- and parabolic-type problems by using the time-independent or time-dependent fundamental solutions, it is still rather difficult to directly solve the wave equations by using the MFS unless we employ the finite difference time-marching scheme to discretize the hyperbolic-type wave equations into the elliptic-type equations (Young, Gu and Fan (2009)) This is because the fundamental solution of wave equation always accompanies with the Dirac delta function (or the Heaviside step function). When the fundamental solution of the wave equation is used directly to implement the MFS, we have to face the difficulty of collocating or differentiating the Dirac delta function (or Heaviside step function) with respect to the time domain for building a linear system. This will result in difficult singularity problems for computer calculation by directly using the MFS.

The other famous process to avoid the singularity of wave fundamental solutions for analyzing the wave problems is to transform the physical variables of wave equations from the time-space domain into the frequency-space domain through the Helmholtz equations, if harmonic waves are allowed. The well-known numerical models such as the desingularized boundary element method (Callsen, Estorff and Zaleski (2004)), the least square-based finite difference method (Shu, Wu and Wang (2005)), the MFS (Young and Ruan (2005)) and RMM (Chen, Chen and Kao (2006)), etc. all were well developed to solve the Helmholtz equations in the frequency domain. As a result time-dependent problems become boundary value problems, however it is sometimes more difficult to directly capture the transient phenomena of the high frequency wave field via this mode decomposition approach.

Another alternative not to use the wave fundamental solutions for solving wave equations is to avoid directly dealing with the Dirac delta function. The D'Alembert solution (Whitham (1974)) is one of the most famous formulas to avoid this kind

of problem in the one-dimensional time-space domain. The D'Alembert formulation combining with the decomposition method was used to obtain the solutions of wave equations in the infinite domain (Wazwaz (1998)). The D'Alembert solution was also combined with the diamond rule, Laplace transform and convolution integral to animate the one-dimensional wave phenomenon (Chen, Chou and Kao (2009)). When the D'Alembert formula is used to transform the wave equation, the wave equation is decomposed into a linear hyperbolic system and becomes easier to implement the initial conditions into the linear system by the ELMFS formulation. The ELMFS has been selected to combine with the D'Alembert formula for directly solving the one-dimensional wave equation (Gu, Young and Fan (2008)), however there exist some difficulties to deal with the finite domain problems.

In this paper, a novel numerical solver based on the ELMFS and the D'Alembert formulation is developed to solve the one-dimensional wave equation with finite and infinite domains. The details of the D'Alembert formulation and the numerical procedure are explained in the following sections. In the section of numerical experiments, the problem of one-dimensional traveling wave propagation is solved to validate the feasibility of the proposed ELMFS. In addition the proposed model is applied to solve two kinds of Cauchy problems in the infinite domain. Moreover the present model is finally adopted to solve the vibration string problems in a finite domain with the fixed and reflection boundaries. All numerical results compare well with the analytical solutions. The conclusions and discussions based on the numerical results are drawn in the last section.

2 Governing Equation

The initial value problem is governed by the wave equation, which can be written as follows.

$$\frac{\partial^2 \varphi}{\partial t^2} = a^2 \frac{\partial^2 \varphi}{\partial x^2}, \quad -\infty < x < \infty, \quad t > 0, \tag{1}$$

where, $\phi(x,t)$ is the physical variable, a is the wave speed, t and x are time and space coordinates, respectively. In Cauchy or initial value problems, the first- and second-kind Cauchy or initial conditions are described as follows.

$$\varphi(x,t)|_{t=0} = f(x) \text{ and } \left.\frac{\partial \varphi(x,t)}{\partial t}\right|_{t=0} = g(x), \tag{2}$$

where the initial conditions $f(x)$ and $g(x)$ are arbitrary given functions.

2.1 The D'Alembert formulation

Replacing the canonical coordinates from (x,t) to (ξ,η), the characteristic coordinates ξ and η are defined as $\xi = x + at$ and $\eta = x - at$. After the integrating

procedures, the general solution of the wave equation can be written as:

$$\varphi(x,t) = \Phi^{+}(x-at) + \Phi^{-}(x+at), \tag{3}$$

where, the general solution φ of the wave equation is separated into two traveling waves Φ^{+} and Φ^{-} in the opposite-directions with the wave speed a. The D'Alembert formula for the initial value problems can be written as the following.

$$\varphi(x,t) = \frac{1}{2}\left[f(x-at) + f(x+at)\right] + \frac{1}{2c}\int_{x-at}^{x+at} g(\sigma)\, d\sigma. \tag{4}$$

According to the D'Alembert formulation, the solution of wave equation can be decomposed as two solutions of advection equations, and the initial conditions can be substituted into these two solutions. It is clearly denoted that the solution of the wave equation is reduced to two opposite-direction advection waves $\Phi^{+}(x-at)$ and $\Phi^{-}(x+at)$ in implicit forms. The definition of the wave motions as the characteristics, Φ^{+} and Φ^{-} must satisfy the pure-advection equation as follows.

$$\frac{D\Phi^{+}}{Dt} = \frac{\partial\Phi^{+}}{\partial t} - a\frac{\partial\Phi^{+}}{\partial x} = 0 \text{ and } \frac{D\Phi^{-}}{Dt} = \frac{\partial\Phi^{-}}{\partial t} + a\frac{\partial\Phi^{-}}{\partial x} = 0. \tag{5}$$

In this study, the term of artificial viscosity is introduced for feasible calculation. The advection equations are therefore rewritten as the advection-diffusion equations:

$$\begin{aligned} \frac{D\Phi^{+}}{Dt} &= \frac{\partial\Phi^{+}}{\partial t} - a\frac{\partial\Phi^{+}}{\partial x} = K\frac{\partial^2\Phi^{+}}{\partial x^2} \\ \frac{D\Phi^{-}}{Dt} &= \frac{\partial\Phi^{-}}{\partial t} + a\frac{\partial\Phi^{-}}{\partial x} = K\frac{\partial^2\Phi^{-}}{\partial x^2}, \end{aligned} \tag{6}$$

where, K is the diffusion coefficient. When the diffusion coefficient becomes an extremely small constant, the advection-diffusion equation is reduced to the pure-advection equation. In other words, the diffusion coefficient K controls the magnitude of the diffusion effect and decides the parabolic- or hyperbolic-type type of the partial differential equation. Following this assumption, the advection-diffusion equation can be easily solved by employing the ELMFS which is based on the diffusion fundamental solution and the ELM.

2.2 Boundary conditions

Boundary conditions of the wave field can be written as the general solution form as equation (3). In other words, there are two opposite-direction traveling wave solutions which must be obtained at the boundary for each time step. However,

there is one characteristic always tracks out of the computational domain and the other characteristic always tracks in the inner domain. The symmetrical concepts are used for dealing the problem of boundary conditions. For satisfying the fixed boundary, the general solution can be written as the following:

$$\Phi^{+}(L-at) = -\Phi^{-}(L+at). \tag{7}$$

For satisfying the no flux boundary, the general solution of the no flux boundary condition can be written as follows:

$$\Phi^{+}(L-at) = \Phi^{-}(L+at). \tag{8}$$

3 Numerical Analysis

3.1 The Eulerian-Lagrangian method

The results of the advection-diffusion equations with convective term can be retrieved from the numerical diffusion results by tracking the massless particles along the characteristic path. In the ELM, the wave speed a is expressed in terms of the spatial and time increments as the compatibility condition as follows:

$$\frac{dx}{dt} = a \Rightarrow x^{n} = x^{n+1} - a\Delta t, \tag{9}$$

In Fig. 1 (b), the line $\overline{P_2P_1}$ is the characteristic path on which transport of the scalar quantity can be traced. If the wave speed at point P_1 is assigned, the spatial location of point P_2 can be traced by Eq.(9). When the spatial location of point P_2 is determined, the solutions along characteristics $\overline{P_2P_1}$ will follow the characteristic-diffusion equation according to the material derivative. After the diffusion process is calculated by the MFS, the solution of the advection-diffusion equation can be obtained directly by ELM. In Fig. 1 (b), points P_2 and P_3 are located at the same spatial position but at different time levels. On the other words, the line $\overline{P_2P_3}$ is the characteristics path for describing pure diffusion phenomena. When we solve the diffusion equation, the diffusive result of point P_2 at $n+1$ level will be calculated in point P_3. If the physical fields have the advection phenomenon, $\overline{P_2P_1}$ is the characteristic path which satisfies the advection phenomenon and the physical value at point P_1 is properly replaced by the diffusion results at point P_3. And then the results of the advection-diffusion equations at $t = (n+1)\Delta t$ thus can be acquired.

3.2 The method of fundamental solutions

The fundamental solution of the diffusion equation is governed by the following equation.

$$\frac{\partial G}{\partial t} = K\nabla^2 G + \delta(x-\varsigma)\,\delta(t-\tau), \tag{10}$$

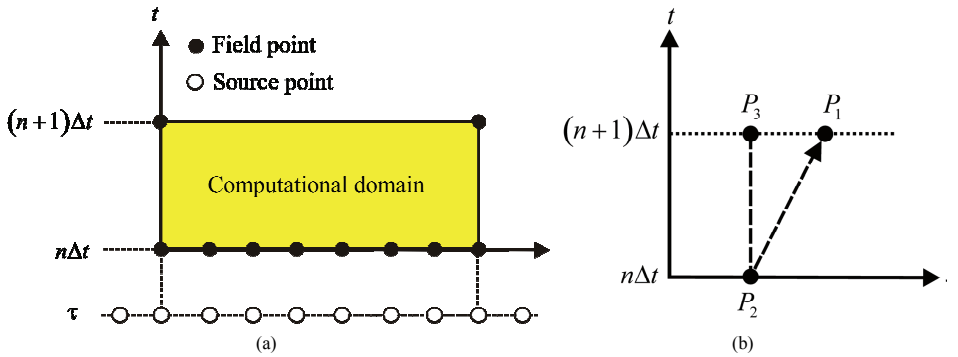

Figure 1: (a) The distribution of field and source points (b) The back-track path along characteristics

where, G is the free-space Green's function (also called the fundamental solution), x and ς are the space-location of field and source points, t and τ are the time coordinates of the field and source points respectively, $\delta()$ is the Dirac delta function. The distributions of field and source points are shown in Fig. 1(a). By taking the integral transforms, the fundamental solution of the diffusion equation can be obtained as the follows.

$$G(x,t;\varsigma,\tau) = \frac{e^{\frac{-(x-\varsigma)^2}{4K(t-\tau)}}}{\left[4\pi K(t-\tau)\right]^{\frac{N_{\dim}}{2}}} H(t-\tau), \tag{11}$$

where, $N_{\dim}$ is the number of dimension of the space and $H()$ is the Heaviside step function. Since the diffusion fundamental solution satisfies homogeneous diffusion equation, the solution of diffusion equation can be assumed as a linear combination of the fundamental solution of diffusion operator. According to the MFS spirit, the numerical solution of the diffusion equation will be written as the following form:

$$F(x,t) = \sum_{j=1}^{M} \alpha_j G(x,t;\varsigma_j,\tau_j), \tag{12}$$

where, M is the number of source points, α_j are the undetermined coefficients or the source intensities in the time-space domain. The linear matrix system can be formed by calculating by the method of collocation through the initial and boundary

conditions.

$$A_{ij}\alpha_j = B_i \text{ and } A_{ij} = \frac{e^{\frac{-\left|x_i-\varsigma_j\right|^2}{4K\left(t_i-\tau_j\right)}}}{\left[4\pi K\left(t_i-\tau_j\right)\right]^{\frac{N_{\dim}}{2}}} H\left(t_i-\tau_j\right), \tag{13}$$

The vector B_i is obtained from the initial and boundary conditions. After solving the linear matrix system, the coefficients α_j can be obtained. Then the solution of diffusion equation can be expressed by Eq. (12).

3.3 The Eulerian-Lagrangian method of fundamental solutions

Following the statement of the ELM and MFS, the solution of the advection-diffusion equation can be written as:

$$F_i^{n+1}(x_i^{n+1},t) = \sum_{j=1}^{M} \alpha_j G\left(x_i^{n+1}-a\Delta t, t; \varsigma_j, \tau_j\right), \tag{14}$$

where, α_j are obtained by calculating the initial and boundary conditions. From Eqs. (11)-(14), the physical value F_i^{n+1} can be easily obtained by the ELMFS. When diffusion effects become very weak (K«1), the advection-diffusion equation can be considered as the advection equation.

3.4 One-dimensional wave model

According to the D'Alembert formulation, the wave equation can be reduced to two solutions of advection equation as $\Phi^+(x-at)$ and $\Phi^-(x+at)$. In mesh-dependent method, it is necessary to use the interpolation technique for back tracking the $\Phi^+(x-a\Delta t)$ and $\Phi^-(x+a\Delta t)$ in time-space domain from level $(n+1)\Delta t$ to level $n\Delta t$. The ELMFS is the suitable meshless method to approximate the solutions as $\Phi^+(x-a\Delta t)$ and $\Phi^-(x+a\Delta t)$ along the characteristics path in the time-space domain with very small diffusion coefficient. After obtaining the solutions $\Phi^+(x-at)$ and $\Phi^-(x+at)$, the solution of wave equation can be calculated as the following.

$$\begin{aligned} & \varphi^{n+1}\left(x_i^{n+1},t\right) = \Phi^+\left(x_i^{n+1}-a\Delta t\right) + \Phi^-\left(x_i^{n+1}+a\Delta t\right) \\ \Rightarrow\ & \varphi^{n+1}\left(x_i^{n+1},t\right) = \sum_{j=1}^{M} \alpha_j G\left(x_i^{n+1}-a\Delta t, t; \varsigma_j, \tau_j\right) + \sum_{j=1}^{M} \alpha_j G\left(x_i^{n+1}+a\Delta t, t; \varsigma_j, \tau_j\right) \end{aligned} \tag{15}$$

Following the definition of the D'Alembert solution and the ELMFS, the numerical procedures of the proposed meshless model are listed below:

1. Set the suitable initial conditions, Eq. (2).
2. Separate the initial conditions for the two opposite-direction traveling waves Φ^+ and Φ^- by the D'Alembert formulation, Eq. (4).
3. Obtain the solutions of two opposite-direction waves by ELMFS, Eqs. (15).
4. Combine the opposite-direction traveling waves by the general solution, Eq. (3), and update the initial condition for next time step.

4 Numerical Experiments

We consider five related numerical experiments to verify the proposed model for solving the one-dimensional wave problems. The numerical examples are analyzed to prove the idea of the proposed numerical method, and show the advantages of the proposed scheme for the infinite and finite domains problems. We will use the root-mean-square error E_{RMS} to measure the accuracy, which is defined as:

$$E_{RMS} = \sqrt{\frac{1}{N_p}\sum_{i=1}^{N_p}\left(\varphi_{i,Numerical} - \varphi_{i,Analytical}\right)^2}. \tag{16}$$

4.1 First-order wave propagation

In the first example, the first-order one-dimensional wave propagation problem is selected to reveal the capability of the proposed ELMFS. In this case, this physical kinematic wave field is governed by the advection or first-order wave equation with the positive unit wave propagation speed as the following:

$$\frac{\partial \varphi}{\partial t} + \frac{\partial \varphi}{\partial x} = 0, \quad -5 < x < 10, \quad t > 0. \tag{17}$$

The initial condition is written as:

$$\varphi(x,t)|_{t=0} = \begin{cases} \sin(x) & -\pi \le x \le \pi \\ 0 & \text{otherwise} \end{cases}, \tag{18}$$

with the following boundary condition:

$$\varphi(x,t)|_{x=-5} = 0. \tag{19}$$

The analytical solution for this problem is shown as follows:

$$\varphi(x,t) = \begin{cases} \sin(x-t) & -\pi \le x-t \le \pi \\ 0 & \text{otherwise} \end{cases}. \tag{20}$$

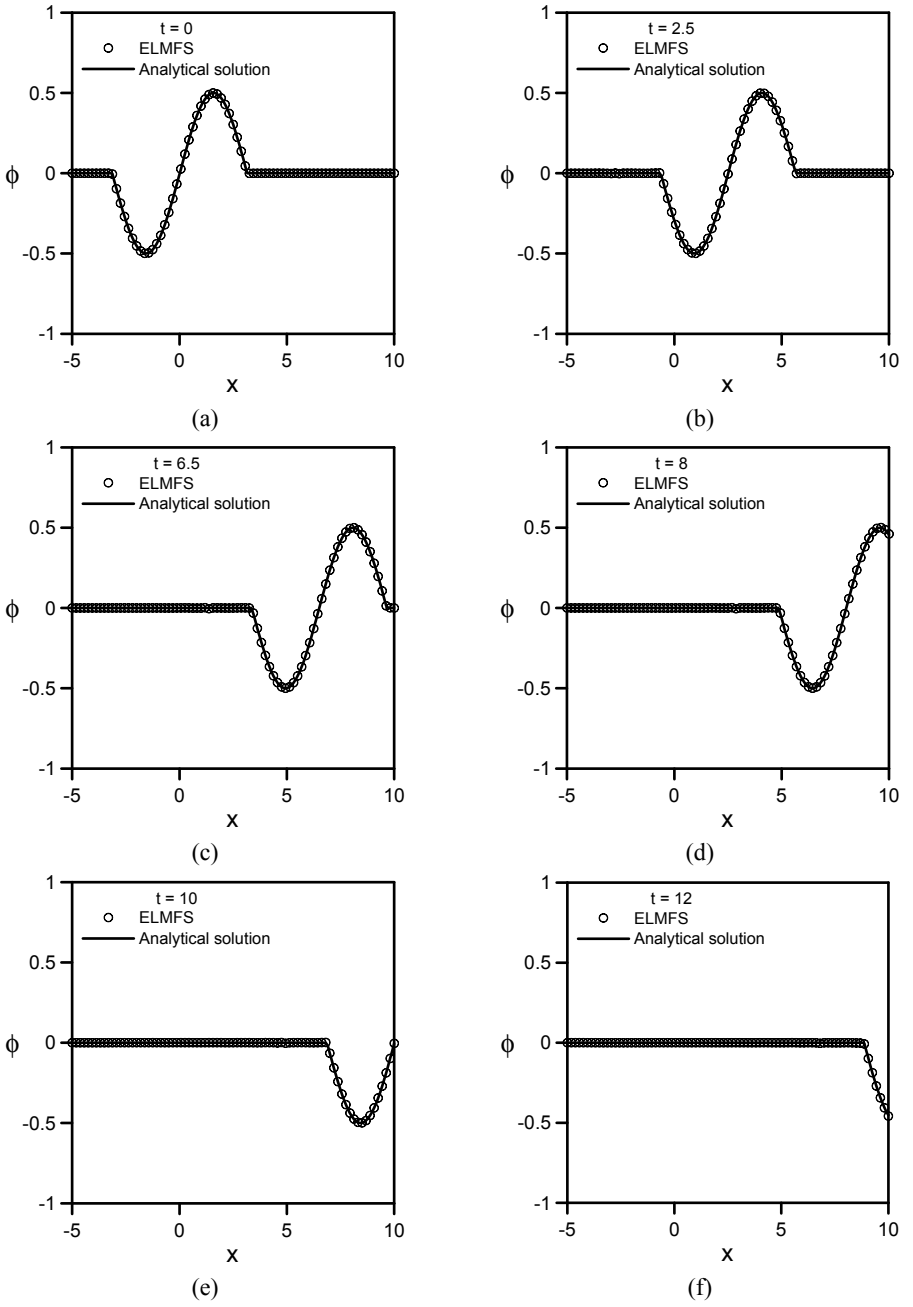

Figure 2: The wave evolution with 161 points of example 4.1 (a) $t = 0$ (b) $t = 2.5$ (c) $t = 6.5$ (d) $t = 8$ (e) $t = 10$ (f) $t = 12$

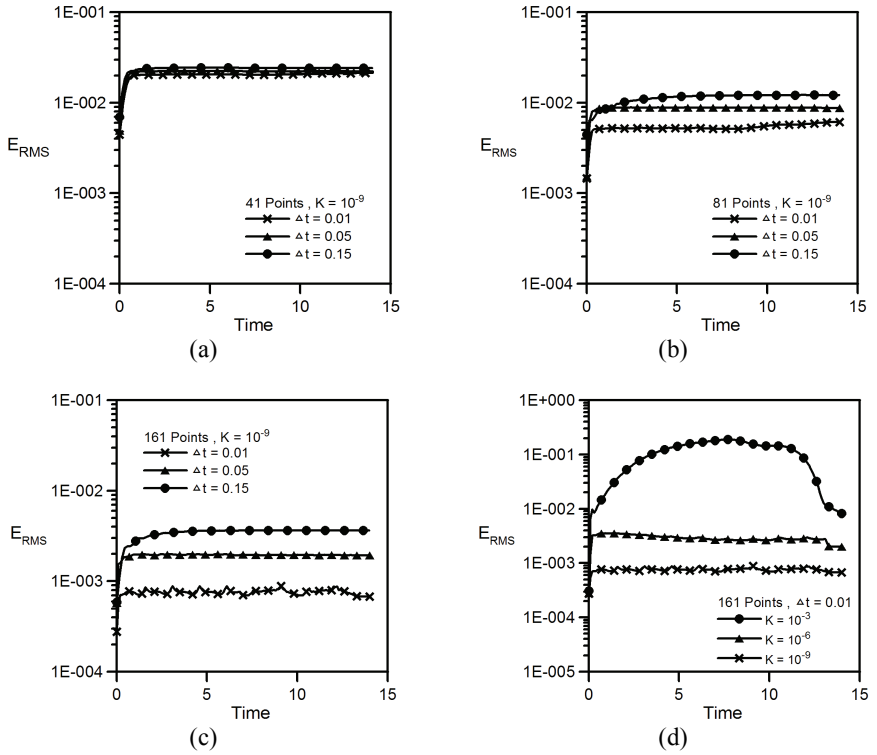

Figure 3: The sensitive test of the wave propagation of example 4.1 (a) 41 points and $K = 10^{-9}$ (b) 81 points and $K = 10^{-9}$ (c) 161 points and $K = 10^{-9}$ (d) 161 points and $\Delta t = 10^{-2}$

In this case, there are two non-smooth points at $x = -\pi$ and $x = \pi$ of the initial condition. When the traveling wave propagates, sometimes the non-smooth position will appear as the non-physical oscillations and which causes the calculation unstable. The uniform point distribution is used for all the sensitivity tests. Figures 2 (a)-(f) depicted the numerical results of the proposed scheme and analytical solution at $t = 0, 2.5,\ 6.5, 8, 10$ and 12. In Figs. 2 (a)-(f), the numerical calculation used 161 points, time-interval $\Delta t = 10^{-2}$ and the diffusion coefficient was selected to be an extremely small constant ($K = 10^{-9}$). Figures 3 (a)-(c) described the dependence of E_{RMS} on different time-interval Δt when 41, 81 and 161 points are used. When the wave passes through the artificial boundary ($x = 10$), the errors still remain at the same order (when $t > 6.5$). From Figs. 3 (a)-(c), it clearly reveals that

as the number of nodes increases, the errors will decrease. In Fig 3 (d), the error curves reveal the diffusion coefficient $K = 10^{-9}$ is small enough to approximate the advection wave propagation phenomenon. In this sensitivity test, the solutions are not sensitive to time-interval (Δt) by the ELMFS. From Figs. 3 (b) and (c), the E_{RMS} are almost smaller than 10^{-2}. In these results, the solutions show consistent behavior.

4.2 The Cauchy problem in infinite domain with zero initial velocity

The one-dimensional Cauchy or initial value problem is selected to demonstrate the capability of the proposed model. The unit wave speed is used in this problem. The initial conditions are considered as a smooth function in infinite computational domain:

$$\varphi(x,t)|_{t=0} = e^{-x^2}, \quad \left.\frac{\partial \varphi(x,t)}{\partial t}\right|_{t=0} = 0, \quad -10 < x < 10. \tag{21}$$

The analytical solution for this problem is displayed as the following.

$$\varphi(x,t) = \frac{1}{2}\left[e^{-(x-t)^2} + e^{-(x+t)^2}\right]. \tag{22}$$

In order to deal with the artificial boundary at $x = -10$ and $x = 10$, the boundary conditions for the Φ^+ and Φ^- can be written as:

$$\Phi^+(x,t)\big|_{x=-10} = 0 \text{ and } \Phi^-(x,t)\big|_{x=10} = 0 \tag{23}$$

Figures 4 (a)-(f) depicted the comparison of numerical results and analytical solution at $t = 0$, 0.5, 1, 1.5, 5 and 7, respectively. The numerical simulation used 161 points for calculation, the diffusion coefficient is set an extremely small constant ($K = 10^{-9}$) and time-interval $\Delta t = 0.05$. Figures 5 (a)-(c) describes the evolution of E_{RMS} with different number of calculation points. In this problem, the errors increase gradually during the set up from $t = 0$ to 1, because the wave is generated in this time framework. Afterward, the waves propagated to the upstream and the downstream and the error curves become stable. In the sensitive tests, the E_{RMS} always decrease when the number of calculation points increases. From Fig. 5 (d), we consider that the diffusion coefficient $K = 10^{-9}$ is sufficiently small to asymptotically reach the pure advection phenomenon. Besides, the time-interval is also not very sensitive to this numerical experiment. From Figs. 5 (a)-(d), the E_{RMS} of the sensitivity tests also displayed the high accuracy of the present scheme for one-dimensional Cauchy or initial value problem.

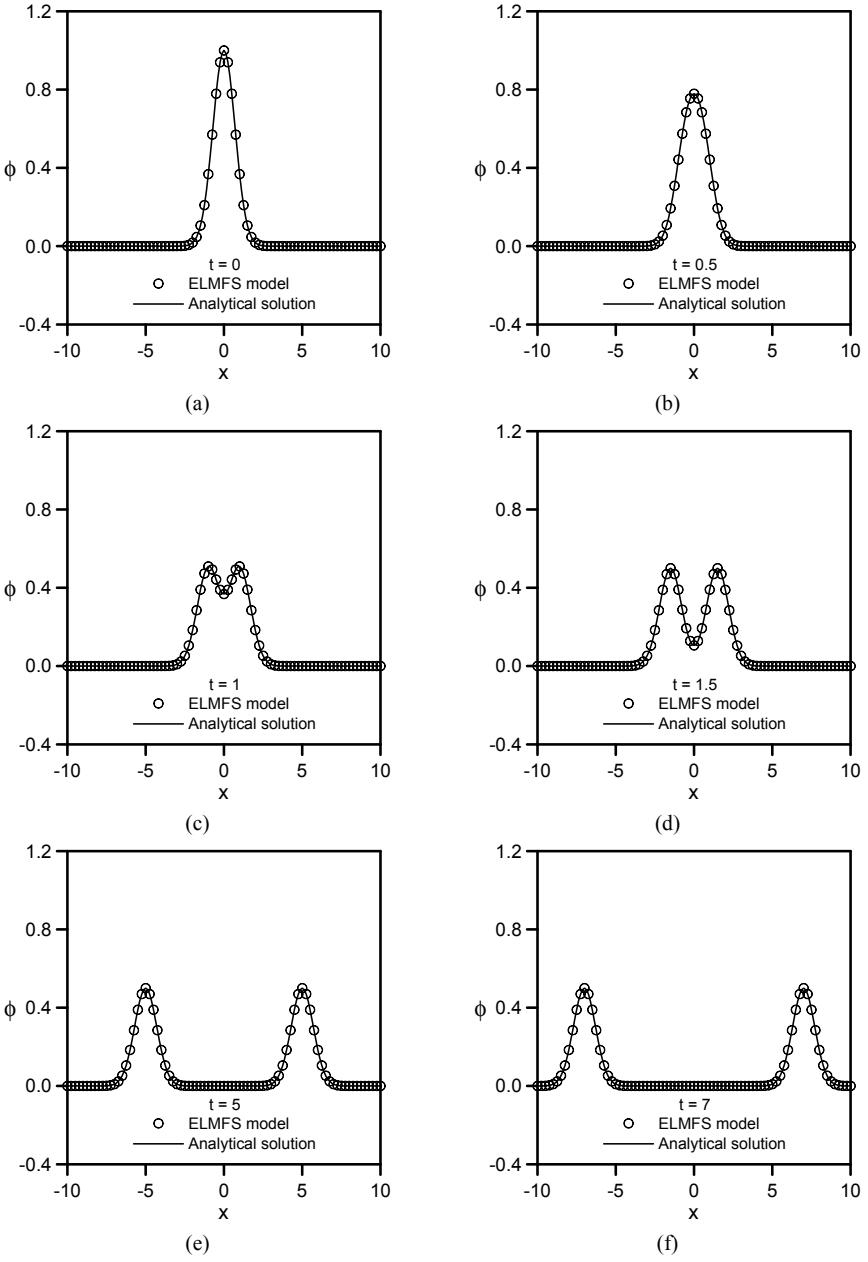

Figure 4: The wave evolution with 161 points,$K = 10^{-9}$ and $\Delta t = 0.05$ of example 4.2 (a) $t = 0$ (b) $t = 0.5$ (c) $t = 1$ (d) $t = 1.5$ (e) $t = 5$ (f) $t = 7$

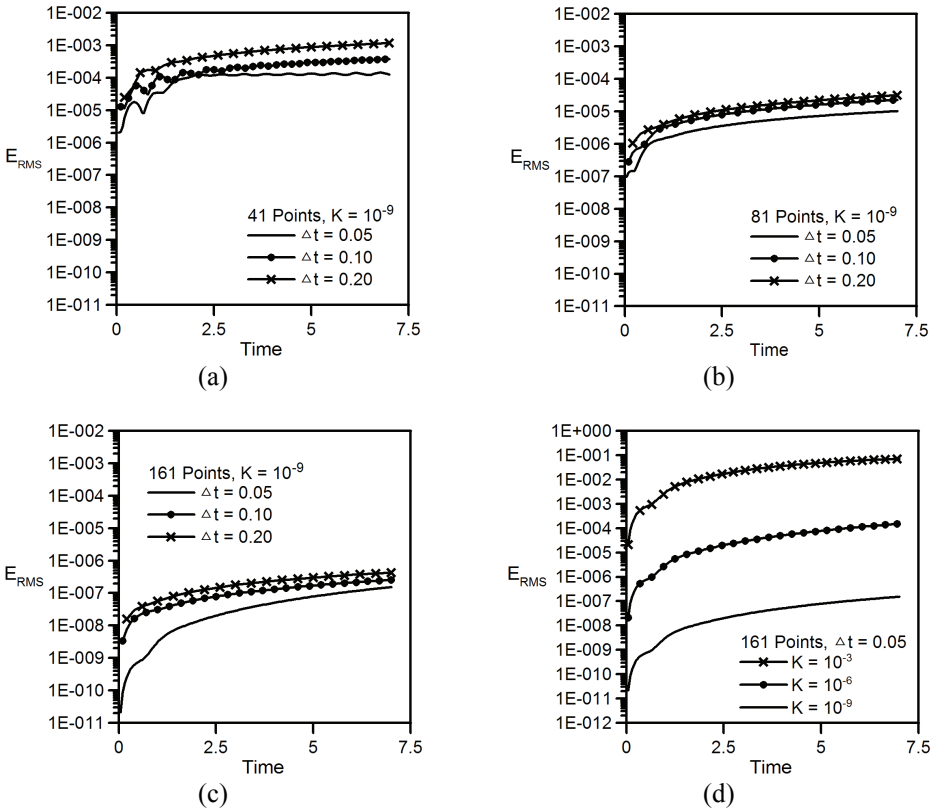

Figure 5: The sensitive test of the Cauchy problem of example 4.2 (a) 41 points and $K = 10^{-9}$ (b) 81 points and $K = 10^{-9}$ (c) 161 points and $K = 10^{-9}$ (d) 161 points and $\Delta t = 0.05$

4.3 The Cauchy problem in infinite domain with zero initial amplitude

In the third test, the one-dimensional Cauchy or initial value problem is selected to express the proposed scheme for dealing with the non-zero second kind initial condition of the wave field. The wave speed a is equal to one for this problem. The initial conditions are selected as a smooth function as the following.

$$\varphi(x,t)|_{t=0} = 0, \quad \left.\frac{\partial \varphi(x,t)}{\partial t}\right|_{t=0} = xe^{-x^2}, \quad -10 < x < 10. \tag{24}$$

The analytical solution for this problem can be written as follows.

$$\varphi(x,t) = \frac{1}{4}\left[e^{-(x-t)^2} - e^{-(x+t)^2}\right]. \tag{25}$$

The artificial boundary conditions at the $x = -10$ and $x = 10$ for Φ^+ and Φ^- are the same as the case 4.2.

Figures 6 (a)-(f) depicts the numerical results and analytical solution at $t = 0$, 0.25, 1, 2, 3.5 and 7.5, respectively. In Fig. 6, the numerical simulation used 161 pints for calculation, the diffusion coefficient is set an excessively small constant ($K = 10^{-9}$) and time-interval $\Delta t = 0.05$. Figures 7 (a)-(c) describe the time evolution history of the E_{RMS} with 41, 81 and 161 calculation points. In this problem, the setup effects lead into the fact that the error suddenly increases during the wave generated in this time interval. Then the error curves become smooth after the waves propagated to positive and negative directions. In the sensitivity cases, the E_{RMS} always decrease when the calculation points number increases. Observing from Fig. 7 (d), it clearly exhibits that the diffusion coefficient $K = 10^{-9}$ is small enough to approximate the solution of advection equations. In addition, the time-interval is also not sensitive to this numerical experiment. From Figs. 6 and 7, the E_{RMS} of the sensitivity cases also show the high accuracy of the proposed scheme for the one-dimensional Cauchy initial value problem.

4.4 The Cauchy problem in bounded domain

In the fourth test, the one-dimensional problem of vibration string is selected to spread out the capability of the proposed model to the finite domain. In this problem, the wave propagation speed is set equal to one in the domain $0 < x < 2$. The initial condition is considered as a parabolic curve in bounded domain as follows.

$$\varphi(x,t)|_{t=0} = x(2-x) \text{ and } \left.\frac{\partial \varphi(x,t)}{\partial t}\right|_{t=0} = 0, \tag{26}$$

while boundary conditions at the $x = 0$ and $x = 2$ are considered as the fixed boundary as follows.

$$\varphi(x,t)|_{x=0} = 0 \text{ and } \varphi(x,t)|_{x=2} = 0. \tag{27}$$

The analytical solution can be obtained by the method of variables separation, which yields:

$$\varphi(x,t) = \frac{32}{\pi^3} \sum_{n=0}^{\infty} \left[\frac{1}{(2n+1)^3} \sin\left(\frac{(2n+1)\pi x}{2}\right) \cos\left(\frac{(2n+1)\pi t}{2}\right) \right]. \tag{28}$$

By using the D'Alembert solution to reduce the wave equations, we depicted the numerical results and to compare with the analytical solution in Figs. 8 (a)-(i) at $t = 0$, 0.5, 1, 1.5, 2, 2.5, 3, 3.5, 4 and 4.5, respectively. We use 41 points for calculation, the diffusion coefficient is set the extremely small constant ($K = 10^{-9}$) and

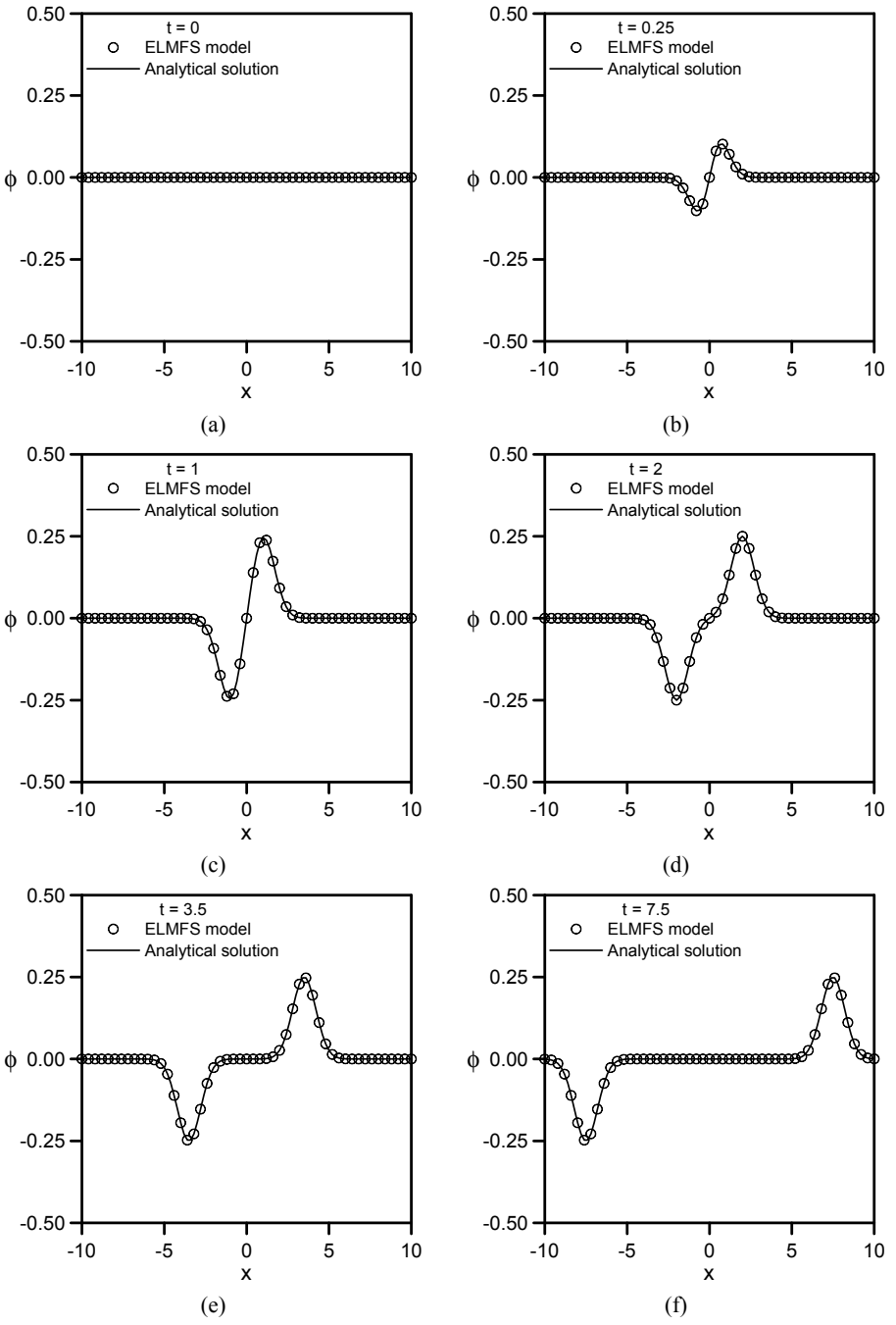

Figure 6: The wave evolution with 161 points, $K = 10^{-9}$ and $\Delta t = 0.05$ of example 4.3 (a) $t = 0$ (b) $t = 0.25$ (c) $t = 1$ (d) $t = 2$ (e) $t = 3.5$ (f) $t = 7.5$

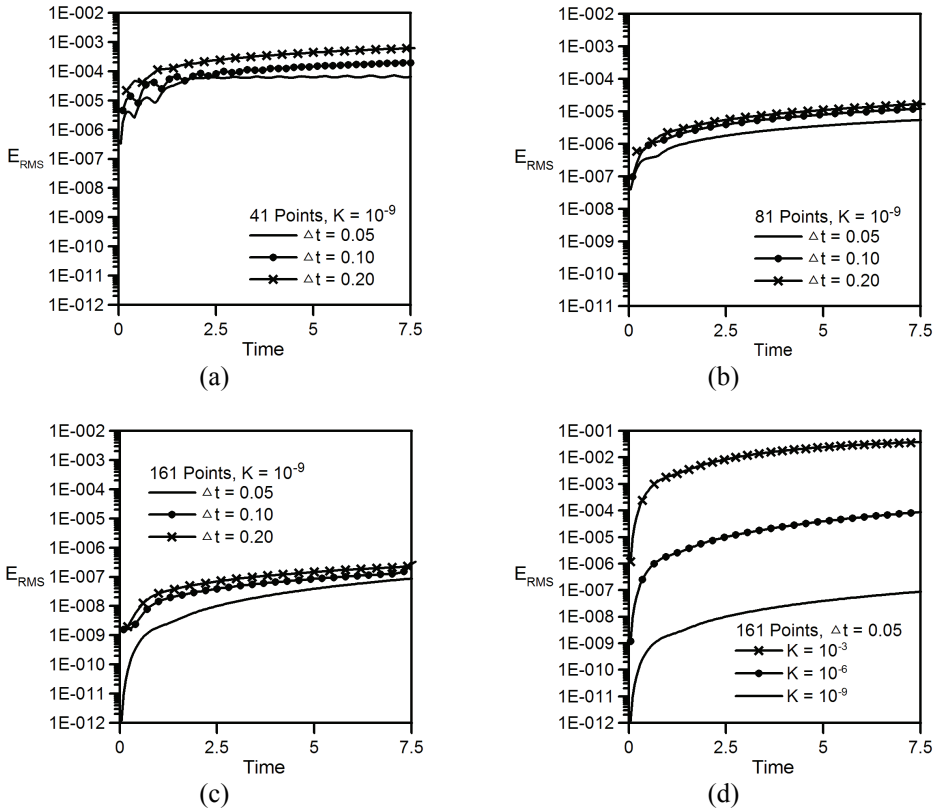

Figure 7: The sensitive test of the wave propagation of example 4.3 (a) 41 points and $K = 10^{-9}$ (b) 81 points and $K = 10^{-9}$ (c) 161 points and $K = 10^{-9}$ (d) 161 points and $\Delta t = 0.05$

$\Delta t = 0.05$. The results compare well with the analytical solution. Figure 9 describes the root-mean-square error for many cycles with stable oscillation. It means that the results of the proposed scheme have high accuracy and very stable.

4.5 The wave vibration problem in the finite domain

In the final test, the one-dimensional wave vibration problem in the finite domain is selected to demonstrate the feasibility of the proposed scheme. In this problem, the wave speed is set as $a = 1$ in the finite domain $0 < x < 1$. The initial conditions are considered as a smooth curve as follows.

$$\varphi(x,t)|_{t=0} = x(x-2) \text{ and } \left.\frac{\partial \varphi(x,t)}{\partial t}\right|_{t=0} = 0, \tag{29}$$

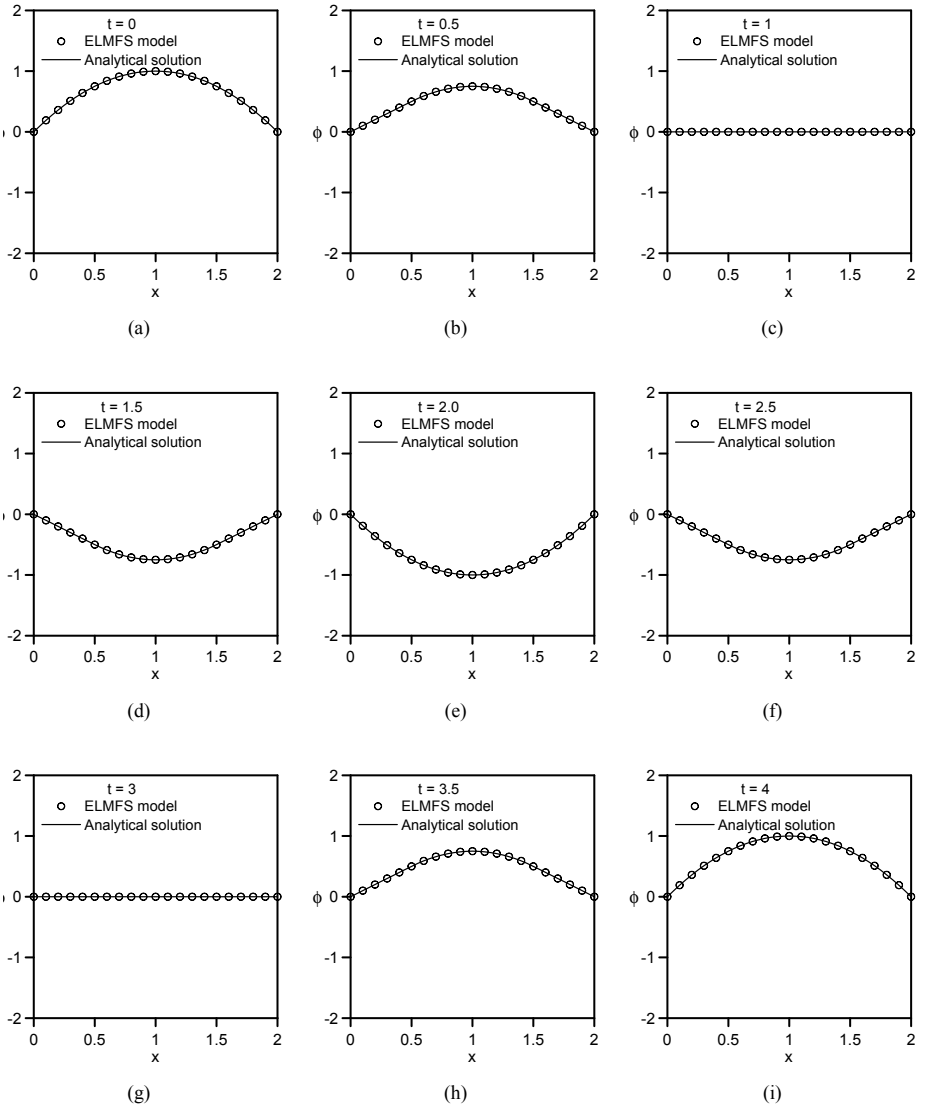

Figure 8: The wave evolution with 41 points, $K = 10^{-9}$ and $\Delta t = 0.05$ of example 4.4 (a) $t = 0$ (b) $t = 0.5$ (c) $t = 1$ (d) $t = 1.5$ (e) $t = 2$ (f) $t = 2.5$ (g) $t = 3$ (h) $t = 3.5$ (i) $t = 4.5$

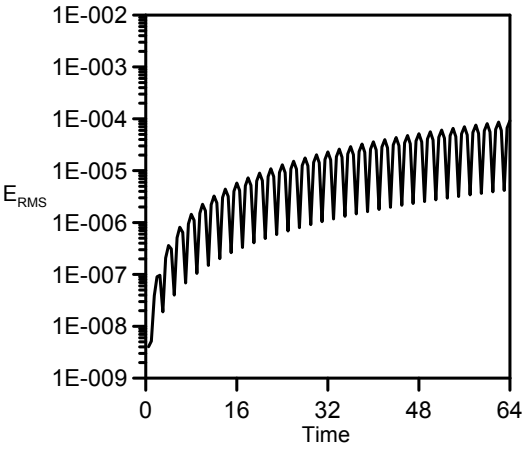

Figure 9: The root-mean-square error of the Cauchy problem in bounded domain of example 4.4

while boundaries at $x=0$ and $x=1$ are considered as the fixed and no flux boundary conditions, respectively as follows.

$$\varphi(x,t)|_{x=0}=0 \text{ and } \left.\frac{\partial\varphi(x,t)}{\partial x}\right|_{x=1}=0. \tag{30}$$

The analytical solution is listed as the following.

$$\varphi(x,t)=-\frac{32}{\pi^3}\sum_{n=0}^{\infty}\frac{1}{\omega_n^3}\sin\left(\frac{1}{2}\omega_n^{\pi}x\right)\cos\left(\frac{1}{2}\omega_n^{\pi}ct\right),\ \omega_n=2n+1. \tag{31}$$

By using the D'Alembert solution to decompose two opposite-direction waves, the numerical results comparing well with the analytical solution are depicted in Figs. 10 (a)-(i) at $t=0$, 0.8, 1, 1.2, 2, 2.8, 3, 3.2 and 4, respectively. The simulation used 26 pints for calculation in this case, the diffusion coefficient is selected to be very small constant ($K=10^{-9}$) and $\Delta t=0.04$. Figure 11 describes the evolution of E_{RMS} for several cycles and the errors are always small than10^{-4}, and it clearly shows that the curves are stably oscillating. We confirm from Figs. 10 and 11, that the proposed meshless model is an excellent numerical scheme.

5 Conclusion

In this paper a novel meshless numerical method based on the MFS and ELM was developed to approximate the solution of one-dimensional wave equations. The

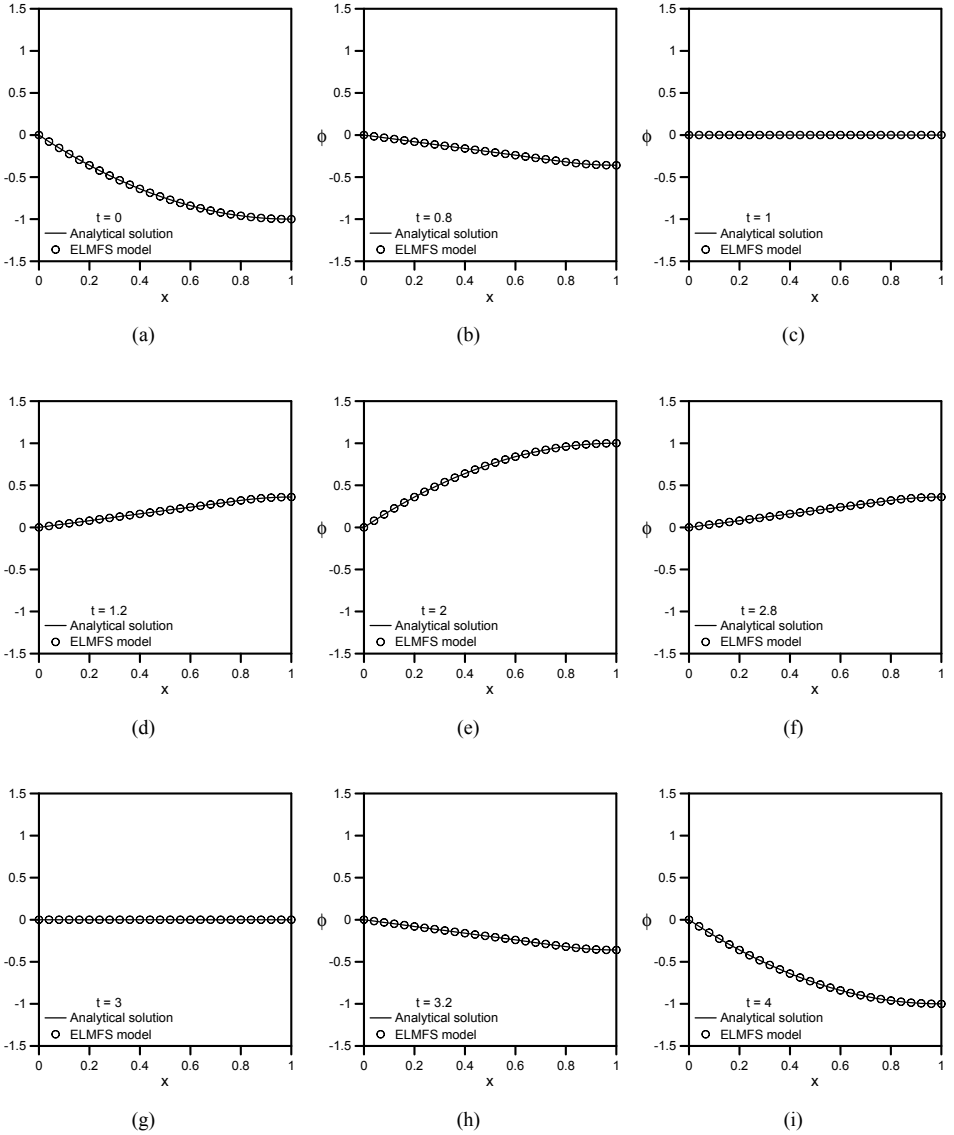

Figure 10: The wave evolution with 26 points, $K = 10^{-9}$ and $\Delta t = 0.04$ of example 4.5 (a) $t = 0$ (b) $t = 0.8$ (c) $t = 1$ (d) $t = 1.2$ (e) $t = 2$ (f) $t = 2.8$ (g) $t = 3$ (h) $t = 3.2$ (i) $t = 4$

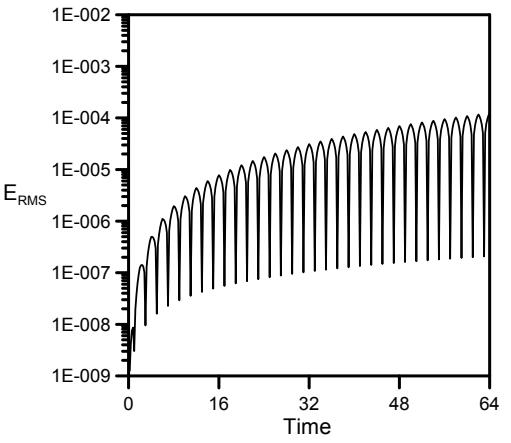

Figure 11: The root-mean-square error of the wave vibration problem in finite domain of example 4.5

proposed model based on the D'Alembert formulation transforms the wave equation into two advection equations in implicit form with the opposite-direction wave speed. The D'Alembert formulation is used to avoid the difficulty of building the linear system of the Cauchy conditions by MFS. The calculation works then pass to the ELMFS which does not need the numerical integration and mesh generation procedures in time-space domain. The solutions of traveling waves are approximated by the system of advection-diffusion equations, the small effects of the artificial diffusion term lead the process of the calculation to be stable and which can easily handle the diffusion effects by the diffusion coefficient. The proposed ELMFS can be easy to transpose the solutions between the Eulerian and the Lagrangian coordinates alone the characteristic path, and the model performs very well for the hyperbolic problems. Furthermore, the present numerical method does not need any extra integral transform to describe the transient phenomena. The wave propagation problem and Cauchy or initial value problems in the infinite domain are simulated by the proposed model. Finally string vibration problems in the finite domain are also simulated by the proposed meshless numerical scheme. Our numerical results compare very well with the analytical solutions. The numerical results demonstrated the accuracy, consistence and feasibility of the proposed numerical model for the one-dimensional wave equation. Even the proposed model selects the D'Alembert formula to solve the one-dimensional wave problems, the same idea combining with other formula can also be extended to the multi-dimensional wave problems. From the numerical tests, it is convinced that

the proposed model is a promising wave solver for engineering applications.

Acknowledgement: We would like to dedicate this paper to celebrating the 60^{th} birthday of Professor Wen-Hwa Chen of the National Tsing-Hua University. The National Science Council (NSC) of Taiwan is gratefully acknowledged for providing the financial support to carry out the present work under the grant nos. NSC-95-221-E-002-406 and NSC-95-2221-E-002-26, it is greatly appreciated.

References

Alves, C. J. S.; Antunes, P. R. S. (2005): The method of fundamental solutions applied to the calculation of eigenfrequencies and eigenmodes of 2D simply connected shapes. *CMC: Computers Materials & Continua*, vol. 2, pp. 251-265.

Amaziane, B.; Naji, A.; Ouazar, D. (2004): Radial basis function and genetic algorithms for parameter identification to some groundwater flow problems. *CMC: Computers Materials & Continua*, vol. 1, pp. 117-128.

Callsen, S.; Estorff, O. V.; Zaleski, O. (2004): Direct and indirect approach of a desingularized boundary element formulation for acoustical problems. *CMES: Computer Modeling in Engineering and Sciences*, vol. 6, pp. 421-429.

Chen, J. T.; Chou, K. S.; Kao, S. K. (2009): One-dimensional wave animation using Mathematica. *Comput Appl Eng Educ*, vol.17, pp.323-339.

Chen, K. H.; Chen, J. T.; Kao, J. H. (2006): Regularized meshless method for solving acoustic eigenproblem with multiply connected domain. *CMES: Computer Modeling in Engineering and Sciences*, vol.16, pp. 27-39.

Chen, K. H.; Chen, J. T.; Kao, J. H. (2008): Regularized meshless method for antiplane shear problems. *Int J Numer Meth Eng*, vol.73, pp.1251-1273.

Chen, K. H.; Kao, J. H.; Chen, J. T. (2009): Regularized meshless method for antiplane piezoelectricity problems with multiple inclusions. *CMC: Computers Materials & Continua*, vol.9, pp.253-279.

Chen, K. H.; Wu, K. L.; Kao, J. H.; Chen, J. T. (2009): Desingular meshless method for solving Laplace equation with over-specified boundary conditions using regularization techniques. *Comput Mech*, vol.43, pp.827-837.

Chen, K. H.; Kao, J. H.; Chen, J. T.; Young, D. L.; Lu, M. C. (2006): Rgularized meshless method for multiply-connected—domain Laplace problems. *Eng Anal Bound Elem*, vol.30, pp.882-896.

Golberg, M. A. (1995): The method of fundamental solutions for Poisson's equation. *Eng Anal Bound Elem*, vol.16, pp. 205-213.

Godinho, L.; Tadeu, A.; Amado Mendes, P. (2007): Wave Propagation around

Thin Structures using the MFS. *CMC: Computers Materials & Continua*, Vol. 5, No. 2, pp. 117-128.

Gou, M. H.; Young, D. L. (2005): Application of the method of fundamental solutions to solve advection-diffusion equations. The Pacific Congress on Marine Science and Technology, Nov. 6-9, 2005, Changhwa, Taiwan.

Gu, M. H.; Young, D. L.; Fan, C. M. (2008): The meshless method for one-dimensional hyperbolic equation. *J Aeronaut Astronaut Aviat (A)*, vol. 40, pp. 63-72.

Han, Z. D.; Atluri, S. N. (2004): A meshless local Petrov-Galerkin (MLPG) approach for 3-dimensional elasto-dynamics. *CMC: Computers Materials & Continua*, vol. 1, pp. 129-140.

Iske, A.; Käser, M. (2005): Two-phase flow simulation by AMMoC, an adaptive meshfree method of characteristics. *CMES: Computer Modeling in Engineering and Sciences*, vol. 7, pp. 133-148.

Kupradze, V. D.; Aleksidze, M. A. (1964): The method of fundamental solutions for the approximate solution of certain boundary value problems. *U.S.S.R. Comput Math Math Phys*, vol.4, pp. 82-126.

Ma, Q.W. (2007): Numerical Generation of Freak Waves Using MLPG_R and QALE-FEM Methods. *CMES: Computer Modeling in Engineering and Sciences*, Vol. 18, No. 3, pp. 223-234.

Mathon, R.; Johnston, R. L. (1977): The approximate solution of elliptic boundary-value problem by method of fundamental solutions. *SIAM J Numer Anal*, vol. 14, pp. 638-650.

Shu, C.; Wu, W. X.; Wang, C. M. (2005): Analysis of metallic waveguides by using least square-based finite difference method. *CMC: Computers Materials & Continua*, vol. 2, pp. 189-200.

Sladek, J.; Sladek, V.; Zhang, C.; Garcia, S. F.; Wunsche, M. (2006): Meshless local Petrov-Galerkin method for plane piezoelectricity. *CMC: Computers Materials & Continua*, vol. 4, pp. 109-117.

Tsai, C.C.; Young, D.L.; Fan, C.M.; Chen, C.W. (2006): Time-dependent fundamental solutions for unsteady stokes problems. *Eng Anal Bound Elem*, vol. 30, pp. 897-908.

Wazwaz, A. M. (1998): A reliable technique for solving the wave equation in an infinite one-dimensional medium. *Appl Math Comput*, vol. 92, pp. 1-7.

Whitham, G. B. (1974): *Linear and nonlinear waves*. John Wiley & Sons press, New York, pp. 214-215.

Young, D. L.; Ruan, J. W. (2005): Method of fundamental solutions for scattering

problems of electromagnetic waves. *CMES: Computer Modeling in Engineering and Sciences*, vol. 7, pp. 223-232.

Young, D. L.; Wang, Y. F.; Eldho, T. I. (2000): Solution of the advection-diffusion equation using the Eulerian-Lagrangian boundary element method. *Eng Anal Bound Elem*, vol. 24, pp. 449-457.

Young, D. L.; Tsai, C. C.; Fan, C. M. (2004): Direct approach to solve nonhomogeneous diffusion problems using fundamental solutions and dual reciprocity methods. *J Chin Inst Eng*, vol. 27, pp. 597-609.

Young, D. L.; Chen, C. S.; Wong, T. K. (2005): Solution of Maxwell's equations using the MQ method. *CMC: Computers Materials & Continua*, vol. 2, pp. 267-276.

Young, D. L.; Chen, K. H.; Lee, C. W. (2005): Novel meshless method for solving the potential problems with arbitrary domain. *J Comput Phys*, vol. 209, pp. 290-321.

Young, D. L.; Chen, C. W.; Fan, C. M. (2008) The method of fundamental solutions for low Reynolds number flows with moving rigid body, in *The method of fundamental solutions-meshless Method*, Eds. C.S. Chen, A. Karageorghis, Y. S. Smyrlis, Dynamic Publishers, USA, pp.181-206.

Young, D. L.; Gu, M. H.; Fan, C. M. (2009) The time-marching method of fundamental solutions for wave equations. *Eng Anal Bound Elem*, vol. 33, pp. 1411-1425.

Young, D. L.; Fan, C. M.; Hu, S. P.; Atluri, S. N. (2008): The Eulerian-Lagrangian method of fundamental solutions for two-dimensional unsteady Burgers' equations. *Eng Anal Bound Elem*, vol. 32, pp. 395-412.

Young, D. L.; Lin, Y. C.; Fan, C. M.; Chiu, C. L. (2009) Method of fundamental solutions for solving incompressible Navier-Stokes problems. *Eng Anal Bound Elem,* vol.33, pp.1031-1044.

Young, D. L.; Tsai, C. C.; Murugesan, K.; Fan, C. M.; Chen, C. W. (2004): Time-dependent fundamental solutions for homogeneous diffusion problems. *Eng Anal Bound Elem*, vol. 28, pp. 1463-1473.

Young, D. L.; Fan, C. M.; Tsai, C. C.; Chen, C. W.; Murugesan, K. (2006): Eulerian-Lagrangian method of fundamental solutions for multi-dimensional advection-diffusion equation. *Int J Math Forum*, vol. 1, pp. 687-706.